International Journal of Mechanical Sciences 81 (2014) 126–136

Contents lists available at ScienceDirect

International Journal of Mechanical Sciences

journal homepage: www.elsevier.com/locate/ijmecsci

Mechanics of anisotropic hierarchical honeycombs

R. Oftadeh [a], B. Haghpanah [a], J. Papadopoulos [a], A.M.S. Hamouda [b], H. Nayeb-Hashemi [a], A. Vaziri [a,*]

[a] Department of Mechanical and Industrial Engineering, Northeastern University, Boston, MA, USA
[b] Mechanical and Industrial Engineering, Qatar University, Doha, Qatar

ARTICLE INFO

Article history:
Received 17 November 2013
Received in revised form
6 January 2014
Accepted 11 February 2014
Available online 18 February 2014

Keywords:
Structural hierarchy
Anisotropy
Honeycombs
Cellular structures

ABSTRACT

Anisotropic hierarchical honeycombs of uniform wall-thickness are constructed by repeatedly replacing each three-edge vertex of a base hexagonal network with a similar but smaller hexagon of the same orientation, and stretching the resulting structure in horizontal or vertical directions to break the isotropy. The uniform overall thickness is then adjusted to maintain the constant average density. The resulting fractal-appearing hierarchical structure is defined by the ratios of replacement edge lengths to the underlying network edge length and also the cell wall angle. The effective elastic modulus, Poisson's ratio and plastic collapse strength in the principal directions of hierarchical honeycombs were obtained analytically as well as by finite element analyses. The results show that anisotropic hierarchical honeycombs of first to fourth order can be 2.0–8.0 times stiffer and at the same time up to 2.0 times stronger than regular honeycomb at the same wall angle and the same overall average density. Plastic collapse analysis showed that anisotropic hierarchical honeycomb has the larger plastic collapse strength compared to regular hierarchical honeycomb of the same order at certain oblique wall angles. The current work provides insight into how incorporating anisotropy into the structural organization can play a significant role in improving the mechanics of the materials structure such as regular or hierarchical honeycombs, and introduces new opportunities for development of novel materials and structures with desirable and actively tailorable properties.

1. Introduction

Materials with structural hierarchy over nanometer to millimeter length scales are found throughout Kingdoms *Plantae* and *Animalia*. Examples include bones and teeth [1,2], nacre (mother-of-pearl) [3], gecko foot pads [4], Asteriscus (yellow sea daisy) [5], *Euplectella sponge* [6], wood [2,7] and water repellent biological systems [8]. The idea of using structural hierarchy in engineering structures and materials goes back at least to Eiffel's Garabit Viaduct and then Tower [9]. More modern examples include polymers [10], composite structures [11–13] and sandwich panel cores [14,15]. The effect of structural hierarchy on mechanical and chemical properties of biological and biomimetic systems has been extensively documented [9–17]. The type and order of the hierarchy and the general organization of these structures play a significant role in their properties and functionality [16,17]. For example, Zhang et al. [16] showed that increasing the level of hierarchy in biological materials increases the toughness but decreases the strength, suggesting that an optimal level of hierarchy could be defined.

Incorporating hierarchy into honeycomb lattice structures has been the focus of a number of studies [15,18–21] and has significance with regard to the application of honeycombs in impact energy absorption and structural protection [22–26], thermal isolation [27] and as the structural core of sandwich panels [28–32]. Recently, a new generation of honeycombs with hierarchical organization was achieved by replacing nodes in the regular honeycomb with smaller hexagons [18,19]. One or two orders of optimized hierarchical refinement offered up to 2 and 3.5 times the in-plane stiffness [18] and almost 2 times the plastic collapse strength [19,20] of conventional honeycomb with the same mass. Majority of these works address the mechanical and thermal properties of isotropic honeycomb structures. However, there are relatively little investigations on the mechanical properties of honeycomb structure with stretched cells resulting in anisotropic honeycomb structures. The present paper extends these previous works by horizontally/vertically 'stretching' or reformulating the underlying hexagonal network prior to the hierarchical refinement steps, so that the developed structure is no longer isotropic (wall thickness is maintained uniform, while being adjusted to have fix overall average density as hierarchy is introduced).

In this work, anisotropic hierarchical honeycombs with various oblique-wall angles are compared to hierarchical conventional honeycombs (with $\theta = 30^{o}$). The stretches not only alter the cell

* Corresponding author.
E-mail address: vaziri@coe.neu.edu (A. Vaziri).

http://dx.doi.org/10.1016/j.ijmecsci.2014.02.011
0020-7403

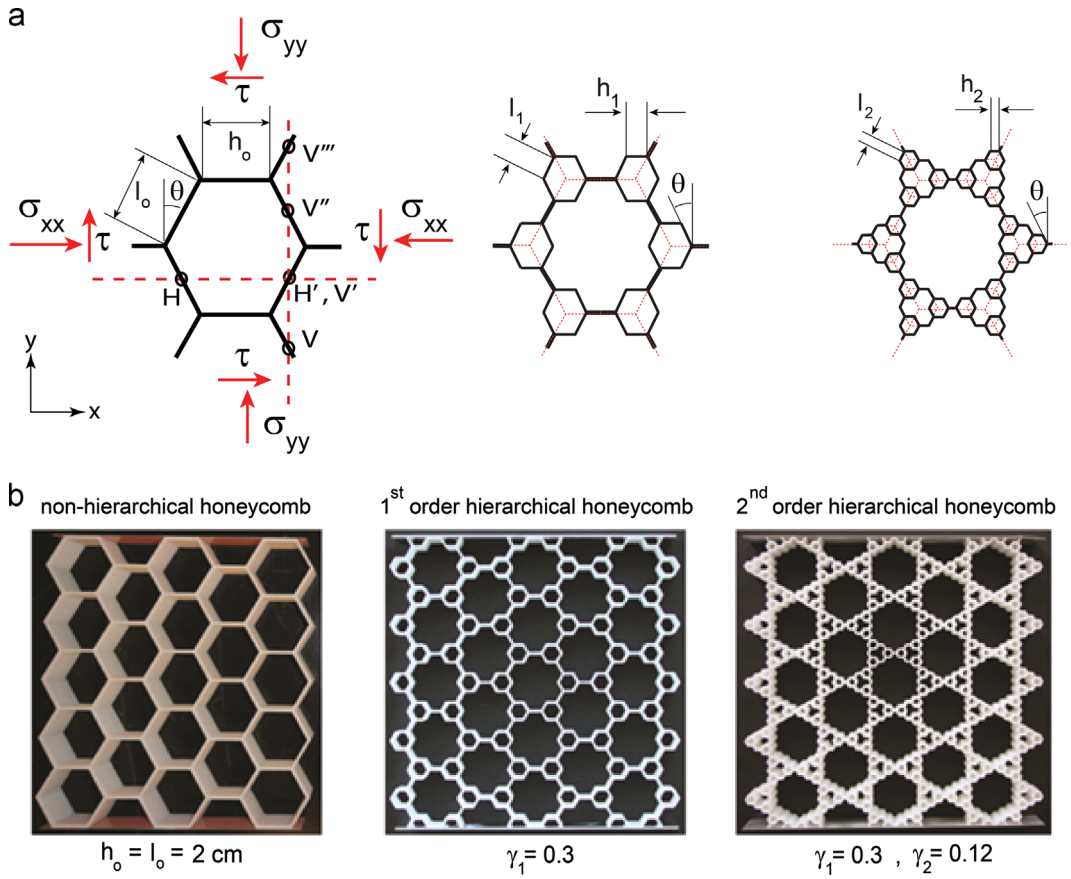

Fig. 1. (a) Sections of the non-hierarchical honeycomb structure (left) and honeycomb structures with one (middle) and two (right) orders of hierarchy. In order for the intersections of newly generated hexagons lie on the edge of previous hexagons, $h_i = 2l_i \sin(\theta)$ for $i = 0, 1, 2, \ldots$ should be satisfied. (b) Images of regular honeycombs with $l_0 = h_0 = 2$ cm fabricated using three-dimensional printing ((b) is taken from [18]).

wall lengths, but it also changes the oblique wall angle, θ (which is equal to 30° in the conventional isotropic honeycomb). Note that uniform stretch leaves oblique cell walls still pointing at the centers of hexagons above and below. Since equal vertical and horizontal stretches would leave the hexagonal geometry undistorted, we 'normalize' the transformation: the length of an oblique cell wall was taken as fixed, while its angle is selected within the range $0 < \theta < \pi/2$. The distorted hexagons of the underlying network therefore have height $2l_0 cos(\theta)$ and horizontal edge length $2l_0 sin(\theta)$ (Fig. 1a). In hierarchically refined structures of uniform thickness, the structural organization is uniquely defined by the ratio of the introduced oblique edge lengths (l_1 and l_2, respectively, for first and second order of hierarchy) to the original hexagon's oblique edge length, l_0. These are denoted $\gamma_1 = l_1/l_0$ and $\gamma_2 = l_2/l_0$, etc., where l_0, l_1, l_2 are defined in Fig. 1a. At each order of hierarchy the introduced *horizontal* edge length conforms to $h_i = 2l_i sin(\theta)$, where l_i is the introduced oblique edge length, θ is the oblique wall angle and h_i is the introduced horizontal edge length.

Here we explore up to four orders of hierarchy. The elastic properties of first and second order hierarchy are evaluated theoretically by Castigliano's method and compared to a matrix frame analysis carried out in MATLAB. The elastic moduli of third and fourth order hierarchy are therefore evaluated numerically only. In Section 2, fabrication of samples using 3D printing is outlined. In Section 3, elastic properties of anisotropic hierarchical honeycombs using Castigliano's second theorem are determined. In section 4, the numerical analysis which carried out in MATLAB is outlined. In Section 5, the effective plastic collapse strength for uniaxial in-plane loading in principal directions is determined using elastic–plastic beam elements in the finite element package ANSYS. In Section 6, results and discussion are demonstrated. In Section 7, conclusions and potential for further performance improvement of hierarchical honeycombs are presented.

2. Fabrication using 3D printing

Fig. 1b shows samples of both zero order and hierarchical *regular*-hexagon honeycombs with relative density of $\bar{\rho} = \rho/\rho_s = 0.10$ and $l_0 = 20$ mm, where ρ is the structural density and l_0 is the oblique hexagon edge length [18]. These samples were fabricated using 3D printing (Dimensions 3D printer, Stratasys Inc., Eden Prairie, MN). The regular honeycomb has $t = 1.75$ mm; the honeycomb with one level of hierarchy has $\gamma_1 = 0.3$ and $t = 1$ mm; and that with two-level hierarchy has $\gamma_1 = 0.3$, $\gamma_2 = 0.12$, and $t = 0.75$ mm, where t is the hexagons wall thickness. These were printed as three-dimensional extruded shells from an ABS polymer (acrylonitrile butadiene styrene, elastic modulus = 2.3 GPa). Fig. 2a shows the images of 1st order anisotropic honeycombs with $\theta = 10^o$, 30^o and 70^o and $l_0 = 2$ cm fabricated using three-dimensional printing. All three structures have $\gamma_1 = l_1/l_0 = 0.3$.

3. Elastic properties of anisotropic hierarchical honeycombs: analytical modeling

Some geometric constraints on the hierarchically introduced edges must be imposed to avoid interfering with pre-existing members: in a honeycomb with first order hierarchy, $0 \le l_1 \le l_0/2$ (Fig. 1a) and thus, $0 \le \gamma_1 \le 0.5$, where $\gamma_1 = 0$ denotes the regular honeycomb structure. For second order hierarchy, the two geometrical constraints are $0 \le l_2 \le l_1$ and $l_2 \le l_0/2 - l_1$. For uniform wall

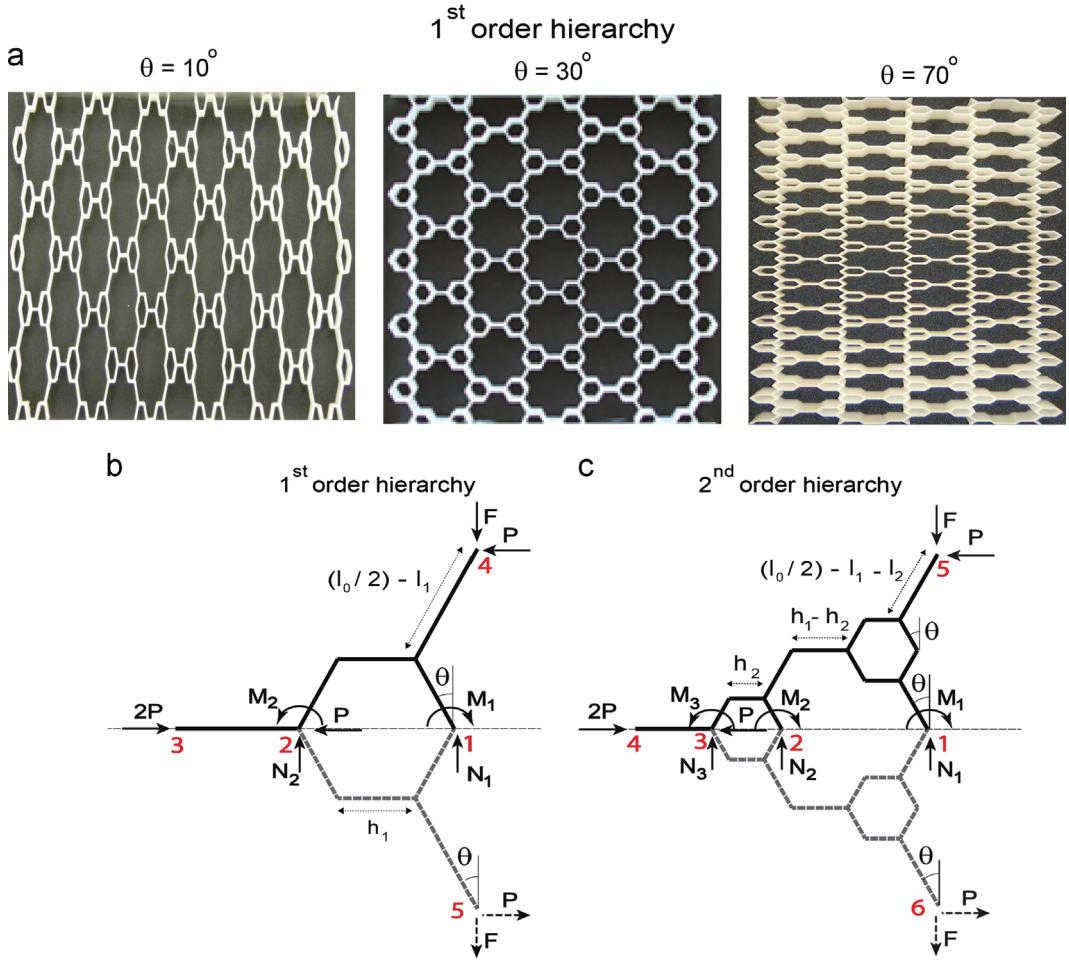

Fig. 2. (a) Images of 1st order honeycombs of $\theta = 10^o$, 30^o and 70^o with $l_0 = 2$ cm fabricated using three-dimensional printing. (b and c) Free body diagrams of the subassembly of hierarchical honeycombs of 1st and 2nd order hierarchy used for finite element and theoretical analysis. N_i and M_i ($i = 1-3$) denote the reaction vertical forces and moments in the edges of the subassembly structures. Note that the solid lines represent the subassembly used for evaluating the elastic modulus/strength, while the whole structure (both dashed and solid lines) is used for shear modulus analyses.

thickness of t, the relative density of the structure (i.e., area fraction) can be given as a function of the length ratios and t/l_0:

$$\frac{\rho}{\rho_s} = \frac{1+\sin\theta}{3\,\sin\theta\,\cos\theta}\left(1+2\sum_{1}^{n} 3^{i-1}\gamma_i\right)\cdot\frac{t}{l_0} \tag{1}$$

where ρ_s is the material density, θ is the oblique wall angle, and n is the hierarchical order. This relation is used to adjust t, so that various choices of θ and γ_i maintain a fixed relative density. A vertical stretch makes the oblique walls much longer than the horizontal walls, as can be seen by letting θ approach 0 in the above expressions (Fig. 2a). In following sections, we mainly focus on results and findings. For detailed description of analytical modeling please refer to Appendix A.

3.1. Elastic modulus in principal directions

The effective elastic modulus (to be normalized by the material elastic modulus, E_s) is defined as the ratio of average stress ($\bar{\sigma}_y = -F/(3l_0 sin\theta)$, $\bar{\sigma}_x = -P/(l_0 cos\theta)$) and average strain ($\bar{\varepsilon}_y = -2\delta_y/(l_0 cos\theta)$, $\bar{\varepsilon}_x = -2\delta_x/(3l_0 sin\theta)$). l_0 is the oblique wall length of the underlying zero-order honeycomb, and θ is the oblique wall angle. P and F are unit-cell boundary points forces in x and y directions, respectively and δ_x and δ_y are the unit-cell boundary point displacements (Fig. 2b and c). The cell walls of thickness t consist of an isotropic elastic material with elastic modulus E_s and Poisson's ratio ν_s. Using the notation $\gamma_1 = l_1/l_0$, the elastic modulus in x and y directions are finally obtained as $E_x/E_s = t^3/l_0^3 \cdot f_x(\gamma_1,\theta)$ and $E_y/E_s = t^3/l_0^3 \cdot f_y(\gamma_1,\theta)$ where

$$f_x(\gamma_1,\theta) = \frac{12\,\sin\theta(\sin\theta+7)/(\cos\theta\,(1-\sin\theta))}{(96\,\sin^2\theta+596\,\sin\theta-148)\gamma_1{}^3+(-48\,\sin^2\theta-168\sin\theta+312)\gamma_1{}^2+(-93\sin\theta-165)\gamma_1+(4\,\sin^2\theta+32\,\sin\theta+28)}$$

and

$$f_y(\gamma_1,\theta) = \frac{4\,\cos\theta(\sin^2\theta+8\,\sin\theta+7)/(3\,\sin^3\theta)}{(192\,\sin^2\theta+644\,\sin\theta-196)\,\gamma_1{}^3+(-96\,\sin^2\theta-192\,\sin\theta+336)\,\gamma_1{}^2+(-93\,\sin\theta-165)\,\gamma_1+(4\,\sin^2\theta+32\,\sin\theta+28)}.$$

These expressions, are valid for any allowable γ_1, in particular for the case when $\gamma_1 = 0$, namely zero order hierarchy. Note also that when $\theta = 30^o$, the resulting isotropy means these expressions should be equal for all values of γ_1.

To find the value of $\gamma_1 = l_1/l_0$ which yields the maximum x or y elastic modulus for a given relative density ρ/ρ_s, Eq. (1) must be used to express t/l_0 as a function of ρ/ρ_s. For the first order of hierarchy, $n=1$, this results in $t/l_0 = 3\ \sin\ \theta\ \cos\ \theta/(1+\ \sin\ \theta)\cdot\rho/\rho_s(1+2\gamma_1)$. (Note that t approaches zero when θ approaches either 0 or 90.) Substituting this into the modulus expressions yields

$$\frac{E_{x,y}}{E_s} = \left(\frac{3\sin\theta\ \cos\theta}{1+\ \sin\theta}\right)^3 \left(\frac{\rho}{\rho_s}\right)^3 f_{x,y}(\gamma_1,\theta)\left(\frac{1}{1+2\gamma_1}\right)^3 \tag{2}$$

where $E_{x,y}$ represents E_x or E_y, and $f_{x,y}$ correspondingly represents f_x or f_y. The analytical tool of MATLAB was used to obtain γ_1 which maximized Eq. (2). A similar procedure can be used to derive elastic moduli of anisotropic honeycomb structures with two orders of hierarchy (Fig. 2c). The elastic moduli in the principal directions were obtained by finding displacements at location of applied forces, F and P. These moduli are function of γ_1, γ_2 and θ and can be presented as: $E_x/E_s = t^3/l_0^3 \cdot f_x(\gamma_1,\gamma_2,\theta)$ and $E_y/E_s = t^3/l_0^3 \cdot f_y(\gamma_1,\gamma_2,\theta)$. To find the optimal values of γ_1 and γ_2 at any constant density ratio ρ/ρ_s, the t/l_0 term is expressed as a function of density ratio ρ/ρ_s. From (1): $t/l_0 = 3\ \sin\ \theta\ \cos\theta/(1+\ \sin\ \theta)/(1+2\gamma_1+6\gamma_2)\cdot\rho/\rho_s$. Substituting this into the elastic modulus expressions yields

$$\frac{E_{x,y}}{E_s} = \left(\frac{3\sin\ \theta\ \cos\ \theta}{1+\sin\ \theta}\right)^3 \left(\frac{\rho}{\rho_s}\right)^3 f_{x,y}(\gamma_1,\gamma_2,\theta)\left(\frac{1}{1+2\gamma_1+6\gamma_2}\right)^3 \tag{3}$$

For the sake of conciseness, both E_x and E_y are shown in one equation with $f_{x,y}$ representing f_x or f_y.

3.2. Effective shear modulus and Poisson's ratio

To fully characterize the linear elastic behavior of horizontally or vertically stretched hierarchical honeycombs, the orthotropic shear modulus G_{xy} and Poisson's ratio ν_{yx} should be obtained as a function of θ and the hierarchical dimension ratios. We applied Castigliano's second theorem to the full subassemblies of Fig. 2b and c to find shear modulus G_{xy} and Poisson's ratio ν_{yx}.

The effective shear modulus (normalized by the material shear modulus G_s) is defined as the ratio of average shear stress $\tau = -P/(3l_0\ \sin\ \theta))$ to average shear strain $(\varepsilon_{xy} = 2\delta_y/(3l_0 sin\theta) + 2\delta_x/(l_0 cos\theta))$. The result can be presented as

$$G_{xy}/G_s = \left(\frac{3\ \sin\ \theta\ \cos\ \theta}{1+\ \sin\ \theta}\right)^3 \left(\frac{\rho}{\rho_s}\right)^3 g_1(\gamma_1,\theta)\left(\frac{1}{1+2\gamma_1}\right)^3 \tag{4}$$

where g_1 is a complex function of γ_1 and θ. For a first-order hierarchical structure the maximum shear modulus occurs when $\gamma_1 = 0.34$, virtually regardless of wall angle θ. However its magnitude depends on θ.

Similarly, for the case of the structure with two hierarchical orders (Fig. 2c), the effective shear modulus can be defined as

$$G_{xy}/G_s = \left(\frac{3\ \sin\theta\ \cos\theta}{1+\ \sin\theta}\right)^3 \left(\frac{\rho}{\rho_s}\right)^3 g_2(\gamma_1,\gamma_2,\theta)\left(\frac{1}{1+2\gamma_1+6\gamma_2}\right)^3 \tag{5}$$

where g_2 is a function of γ_1, γ_2 and θ. Differentiating (5) with respect to $\gamma_1 = l_1/l_0$ and $\gamma_2 = l_2/l_0$ at constant density shows that the maximum normalized shear modulus occurs at $\gamma_1 = l_1/l_0 = 0.3$ and $\gamma_2 = l_2/l_0 = 0.14$.

The Poisson's ratio ν_{yx} can then be obtained from $\nu_{yx} = \delta_x/(3\tan(\theta)\delta_y)$, which results in

$$\nu_{yx} = -\frac{\begin{array}{l}-\cos^2\theta((-112\sin^2\theta - 564\ \sin\theta + 196)\gamma_1{}^3 \\ +(72\sin^2\theta + 180\ \sin\theta - 324)\gamma_1{}^2 + (93\ \sin\theta + 165\gamma_1)\gamma_1 - 4\sin^2\theta - 32\ \sin\theta - 28)\end{array}}{\begin{array}{l}3\sin^2\theta((192\sin^2\theta + 644\ \sin\theta - 196)\gamma_1{}^3 \\ +(-96\sin^2\theta - 192\ \sin\theta + 336)\gamma_1{}^2 + (-93\ \sin\theta - 165)\gamma_1 + 4\sin^2\theta + 32\ \sin\theta + 28)\end{array}}. \tag{6}$$

Performing the same procedure for the second order hierarchy structure of Fig. 2b, we can obtain ν_{yx} as a function of oblique wall angle θ, γ_1 and γ_2 (i.e., $\nu_{yx} = \nu_{yx}(\theta,\gamma_1,\gamma_2)$).

4. Elastic analysis: numerical simulation

To explore the effect of hierarchical order greater than 2, a matrix frame analysis procedure was implemented in MATLAB. Shear and stretching were included in the governing equations for each beam [33]: $d/dx(A\cdot E_s\cdot du/dx) = 0$ for stretching, $d/dx[k_s\cdot A\cdot G_s(dv/dx-\phi)] = 0$ for shearing, and $d/dx(E\cdot I\cdot d\phi/dx) + k_s\cdot A\cdot G_s(dv/dx-\phi) = 0$ for bending, where A is the cross sectional area, I is the second moment of area, E_s and G_s are the elastic and shear moduli of the cell wall material, k_s is the shear coefficient (equal to 5/6 for a rectangular cross section [33]), u, v are the longitudinal and transverse displacements, and ϕ is the beam cross-section rotation about the z-axis. Transformation matrix is calculated for each beam to transform its stiffness matrix to global coordinates and points 3 and 4 were clamped in Fig. 2b and c, respectively. This program was highly efficient and allowed us to systematically change geometry of the hierarchical structure in order to find unique geometry which maximized desired mechanical properties. Compared to the commercial FEA software, the developed program was faster and more flexible. We explored the whole range of γ to determine the elastic modulus range at each hierarchical order.

5. Plastic collapse strength analysis

In this section, Finite Element simulation is performed to study the in-plane uniaxial plastic collapse strength of hierarchical honeycombs with up to four orders of hierarchy. Using beam element, a subassembly of the structure, as defined in Fig. 2b and c, was modeled in ANSYS. The modeled structure was then meshed using plastic 2D cubic beam element (Beam 23) with plastic, creep, and swelling capabilities. Elastic-perfectly plastic behavior was assigned to the chosen material, and element length was taken as $l_0/500$, where l_0 is the length of an oblique wall (short elements are needed to capture localized plastic hinges). The simulations were performed with uniaxial loading separately applied in x and y directions. The elastic modulus, Poisson's ratio and yield strength of material used in the simulations were $E_S = 70$ GPa, $\nu = 0.3$ and $\sigma_y = 130$ MPa, respectively. The relative density of the structure used for plastic collapse strength analysis was 0.01.

The modeled subassembly of the structure was subjected to compressive displacement-controlled loading (i.e., on the points

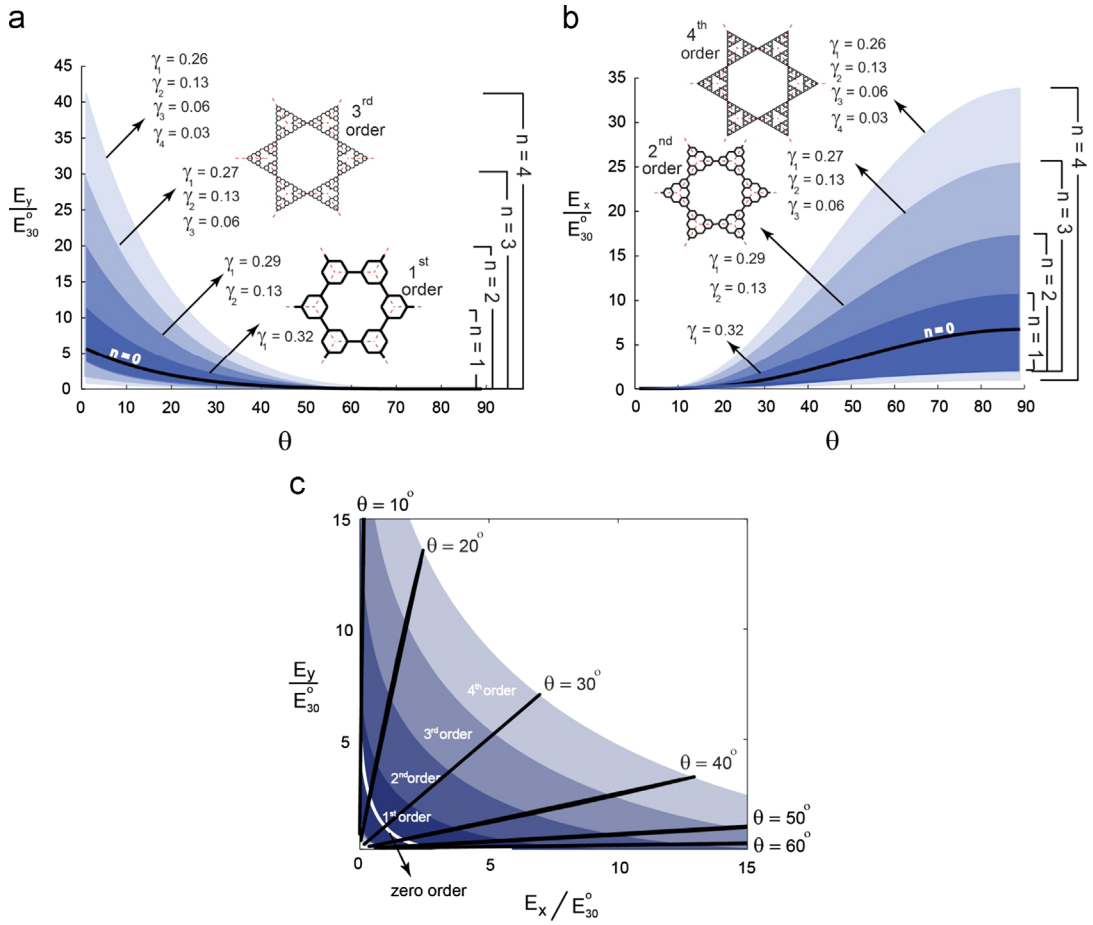

Fig. 3. (a and b) The elastic modulus bandwidth of specific 1st–4th order hierarchical honeycombs, normalized by the zero-order modulus of isotropic honeycomb (i.e., 30° wall angle) for y and x direction. (c) Surface plot of maximum x-direction and y-direction normalized elastic modulus of zero to fourth order hierarchical honeycomb.

4 and 5 in Fig. 2b and points 5 and 6 in Fig. 2c) with free transverse expansion. Strength was defined as the stress associated with the plateau level in the force–displacement curve. The values of collapse strength in each direction are denoted by $S_{y,\theta}$ and $S_{x,\theta}$, where x or y denotes the strength direction and θ is the oblique wall angle.

6. Results and discussion

6.1. Elastic modulus properties

Fig. 3a and b shows the achievable elastic modulus range in the y and x directions as a function of wall angle, for up to 4 hierarchical orders. The computed orthotropic elastic moduli are normalized by the isotropic elastic modulus of zero order unstretched honeycomb (i.e., E^0_{30}). As can be seen from these two figures, by increasing θ, elastic modulus in the y-direction decreases to zero, while normalized x-direction modulus (E_x/E^0_{30}) increases to approximately 6. (The opposite behavior is seen as θ decreases to zero.) These results are explained by the fact that as θ approaches either 0 or 90, beam thickness reduces and bending stiffness rapidly approaches zero. In contrast axial stiffness contribution increases resulting in an overall finite modulus.

Fig. 3a and b also shows that as hierarchical order is increased, not only the maximum elastic modulus but also the elastic modulus range covered by each additional order increases. Values of γ for maximum elastic modulus at each hierarchical order are provided in the figures. These values are approximately independent of θ and the selection of x or y. For third order hierarchy we found $\gamma_1 = 0.27$, $\gamma_2 = 0.13$, $\gamma_3 = 0.06$ and for fourth order we found $\gamma_1 = 0.26$, $\gamma_2 = 0.13$, $\gamma_3 = 0.06$, $\gamma_4 = 0.03$. The trend in γ values suggests that when increasing the hierarchical order, the inserted edge length which gives the stiffest structure tends to be half the edge length of the previous hexagons (i.e., $\gamma_{i+1} = \gamma_i/2$).

Fig. 3c compares normalized elastic moduli in the x- and y-directions (E_y/E^0_{30} versus E_x/E^0_{30}). The θ-constant contours in this figure are shown with solid lines. As can be seen from the figure, by increasing the order of hierarchy (n) the covered area of the map increases. Also, for $\theta < 30^o$ the value of E_x/E^0_{30} is less than E_y/E^0_{30} so that for $\theta < 10^o$ the value of E_x/E^0_{30} is negligible compared to E_y/E^0_{30} and for $\theta > 60^o$ the opposite is true. Therefore the design region for bi-axial loading should be within the range of $15^o < \theta < 50^o$.

In order to understand the effect of hierarchical structure on the elastic moduli of the structure, the elastic modulus for various hierarchical structure are normalized respect to elastic moduli of the non-hierarchical structure for various wall angle θ. Fig. 4a and b shows the x and y elastic moduli of a first-order hierarchical structure, now normalized by $E^o_{x,\theta}$ and $E^o_{y,\theta}$, the non-hierarchical structure of the same wall angle, using data shown by a dark line in Fig. 3a and b. Here we divided the stiffness by the stiffness of the zero order value at the same wall angle θ, unlike Fig. 3 in which it is divided by a constant (E^0_{30}). Surprisingly, the maximum normalized elastic moduli occur in a very narrow range of $\gamma_1 = 0.3147 - 0.3232$ as θ varies from 0 to 90. At $\gamma_1 = l_1/l_0 = 0.32$, $E_y/E^o_{y,\theta} = 2(\sin^2\theta + 8\sin\theta + 7)/(1.02\sin^2\theta + 8.12\sin\theta + 7.02) \approx 1.98$, which varies less than 1% over the entire

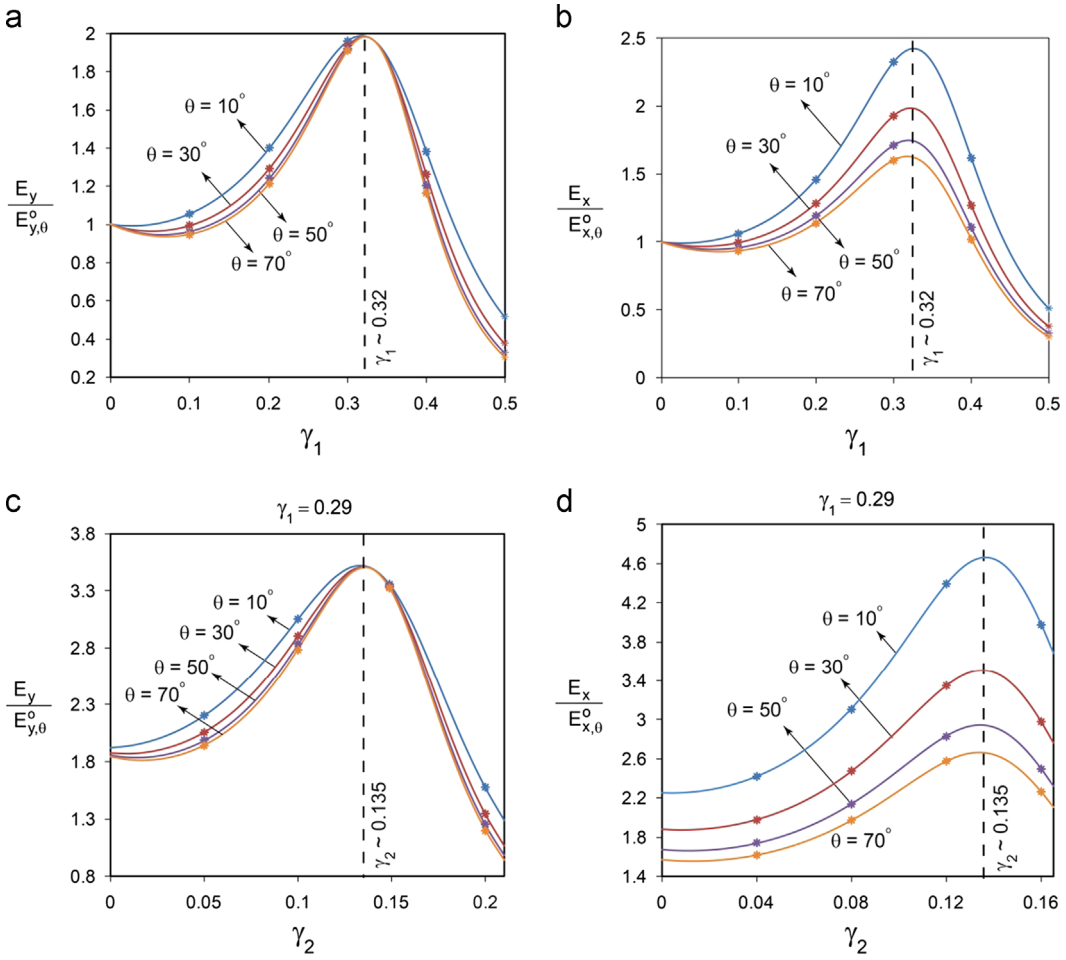

Fig. 4. (a and b) Normalized elastic moduli of 1st order hierarchical honeycomb for y and x direction. (b and c) Normalized elastic moduli of 2nd order hierarchical honeycomb with $\gamma_1 = 0.29$, at y and x direction. The elastic moduli is normalized by that of zero order honeycomb with the same oblique wall angle θ. Data markers are the numerical frame analysis results. Note that E_x and E_y are the same for $\theta = 30^o$.

range of wall angle θ. The maximum elastic modulus in the y-direction for the first order honeycomb is thus about twice that of non-hierarchical honeycomb with the same density ratio, for all θ angles. In contrast, while the x-direction peak elastic modulus occurs for essentially the same hierarchical structure (same choice of γ_1), its value does depend significantly on anisotropy, i.e., θ. Both x and y results clearly show that hierarchical refinement with in some range of γ values always increase elastic modulus (i.e., exceed 1.0), regardless of the wall angle.

The data markers in Fig. 4 show the results of computational analyses on the upper half of the subassembly defined in Fig. 2b and c. They represent the MATLAB frame analysis results for four different oblique wall angles and five different γ_1. The results were obtained by clamping point 3 in Fig. 2b and allowing points 1 and 2 to move horizontally due to structural symmetry. Similarly in Fig. 2c, point 4 was clamped and points 1, 2 and 3 were confined to move horizontally. The frame computation results show good correlation with the theoretical results (maximum error $< 1\%$). The analytical results were based on using bending energy only. In contrast frame analysis was based on considering all deformation energies, (bending, shear and stretching). The agreement could be justified by considering that the bending energy is dominant energy for small relative density of less than 0.01.

Fig. 4c and d shows the normalized elastic modulus for second order hierarchy in the y- and x-directions. The results for the first order hierarchy can be inferred from the plots in Fig. 4a and b at $\gamma_2 = 0$. The derivatives of (3) with respect to $\gamma_1 = l_1/l_0$ and $\gamma_2 = l_2/l_0$ at constant density show that the maximum normalized elastic modulus in the x- and y-directions occur at $\gamma_1 = l_1/l_0 = 0.29$ and $\gamma_2 = l_2/l_0 = 0.135$, respectively (virtually independent of θ), where $E_y/E^o_{y,\theta} \approx 3.52(\rho/\rho_s)^3$. As can be seen in Fig. 4c, the maximum normalized elastic modulus in y-direction for $\gamma_1 = 0.29$ and for all different oblique wall angles is the same. The maximum elastic modulus in the y-direction is almost four times greater than the elastic modulus of a regular honeycomb structure with the same density ratio. In contrast, the maximum normalized elastic modulus in the x-direction depends on the wall angle θ. There is also a good correlation between frame analysis results and theoretical results (maximum error $< 1\%$).

6.2. Shear modulus and Poisson's ratio

Based on the numerical frame analysis in MATLAB, Fig. 5a shows the shear modulus bandwidth (G_{xy}/G^0_{30}) of the structure versus oblique wall angle, θ for up to 4 hierarchical orders, where G^0_{30} is the shear modulus of zero order isotropic honeycomb ($\theta = 30^o$). Fig. 5a shows that by increasing hierarchical order, the possible range of shear modulus increases and the maximum shear modulus is also increases. The oblique wall angle for the maximum shear modulus is approximately $\theta = 28^o$, for all hierarchical orders. Values of γ for maximum modulus at each hierarchical order are virtually independent of θ. For third order hierarchy this occurs at $\gamma_1 = 0.27$, $\gamma_2 = 0.13$, $\gamma_3 = 0.06$, and for the fourth order at $\gamma_1 = 0.27$, $\gamma_2 = 0.13$, $\gamma_3 = 0.06$, $\gamma_4 = 0.03\gamma_3 = 0.06$, $\gamma_4 = 0.03$. The enhancement in

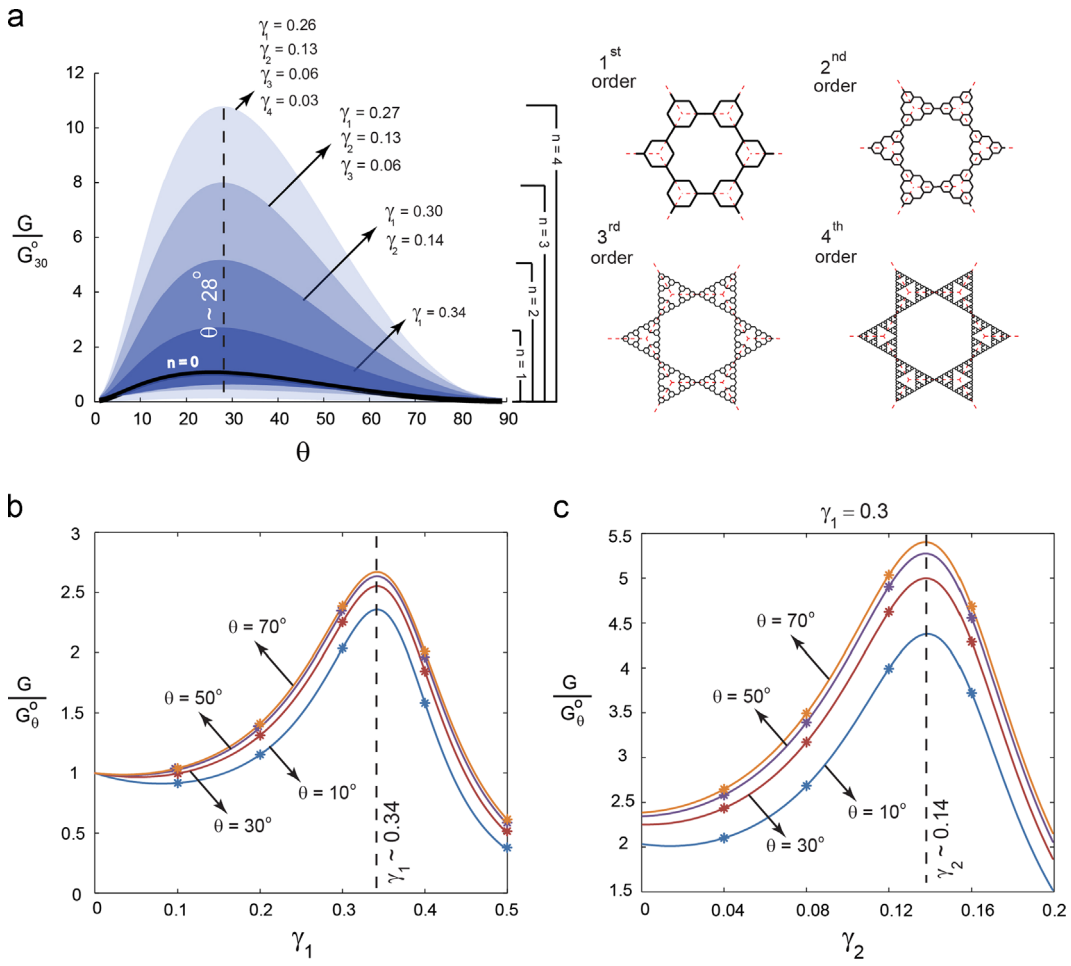

Fig. 5. (a) The normalized shear modulus bandwidth of 1st–4th order hierarchy. (b and c) Normalized shear modulus of 1st and 2nd order hierarchy versus γ_1 and γ_2, respectively. For (a) the shear modulus is normalized by that of zero order regular honeycomb ($\theta = 30^o$), whereas for (b) and (c) it is normalized by that of zero order honeycomb with the same oblique wall angle θ; Data markers are the MATLAB frame analysis results.

the normalized shear modulus is noticeable as it increases from 2.59 and 5.04 for 1st and 2nd order hierarchical honeycombs to 7.87 and 10.78 for 3rd and 4th order. Just as in the previous section on the effect of hierarchical order on the elastic modulus, the trend in γ values which maximized the shear modulus tends to be half the edge length of the previous hexagons (i.e., $\gamma_{i+1} = \gamma_i/2$). Frame analysis results are also shown which were obtained by applying the same loading conditions as those in the analytical analysis.

Fig. 5b shows the shear modulus for first order hierarchical structures, normalized by the modulus of the zero order structure with that same angle. As the oblique wall angle increases, the normalized shear modulus (G_{xy}/G^o_θ) is increased slightly. When $\gamma_1 = 0.34$, the shear modulus of the first order hierarchical honeycombs increases two times of the non-hierarchical honeycombs regardless of wall angle.

Fig. 5c shows the normalized shear modulus for second order hierarchical structure. The maximum normalized shear modulus is moderately dependent on oblique wall angle θ. Trends are the same as those for structures with first order hierarchy. Adding the second order of hierarchy makes the shear modulus almost 2 times greater than for first order hierarchy.

Fig. 6a shows the Poisson's ratio of 1st order hierarchical honeycomb normalized by the Poisson's ratio of zero order honeycomb structure at the same wall angle, θ (i.e., $\nu^o_{yx,\theta} = \cos^2\theta/(3\sin^2\theta)$). For isotropic honeycomb ($\theta = 30^o$) and $\gamma_1 = 0$, ν_{yx} is equal to one. This can be attributed to the deformation of these structures under hydrostatic pressure. Under hydrostatic loading, beams in these structures experience only axial loading. Since these beams are assumed to be inextensible, the Poisson's ratio should be equal to one. However, for honeycomb with other values of oblique wall angle, 2D hydrostatic loading results in a different loading in beams, and thus different values for Poisson's ratio. Furthermore, any hierarchical replacements lead to beam bending (hence strain) so Poisson's ratio must be reduced. It was found, $\nu_{yx}/\nu^o_{yx,\theta} \cong 0.5$ at $\gamma_1 = 0.5$ for all values of θ, with the minimum value of 0.39 for $\theta = 10^o$ and 0.33 for $\theta = 70^o$ at $\gamma_1 = 0.4$. Fig. 6b shows the normalized Poisson's ratio of 2nd order hierarchical honeycomb (i.e., $\nu_{yx}/\nu^o_{yx,\theta}$) in y-direction with $\gamma_1 = 0.29$ versus γ_2 for different values of oblique wall angle, θ. The value of $\nu_{yx}/\nu^o_{yx,\theta}$ is between 0.74 and 0.78 at $\gamma_2 = 0$ and between 0.35 and 0.38 at $\gamma_2 = 0.21$, with the minimum value between 0.29 and 0.34 at $\gamma_2 = 0.17$. As can be seen from these two figures, the curves intersect at a point which correspond to locations in which maximum elastic modulus occurs (i.e., $\gamma_1 = 0.32$ for the 1st order and $\gamma_1 = 0.29$, $\gamma_2 = 0.135$ for 2nd order). Frame computations in MATLAB are also provided for comparison with the analytical solution. The results show a good agreement between analytical results and the frame analysis. Although the frame analysis considered all deformation modes in the structural components, analytical and frame analysis are in good agreement because bending energy is the dominant energy for low density structures.

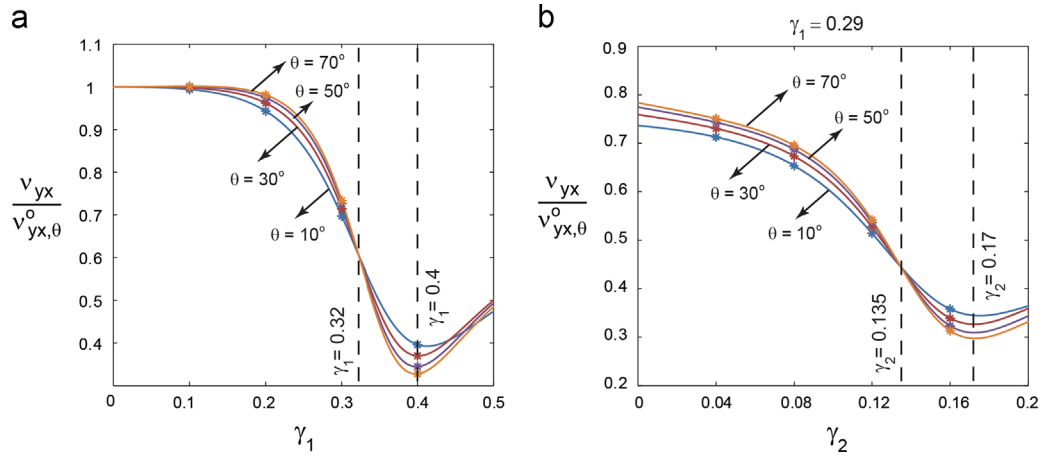

Fig. 6. (a) Poisson's ratio of 1st order hierarchical honeycomb in y-direction versus γ_1 for different values of oblique wall angle, θ. (b) Poisson's ratio of 2nd order hierarchical honeycomb in y-direction with $\gamma_1 = 0.29$ versus γ_2 for different values of oblique wall angle, θ. Star points are the numerical frame analysis results. Note that the results are normalized by non-hierarchical Poisson's ratio at the same angle, which varies significantly with anisotropy.

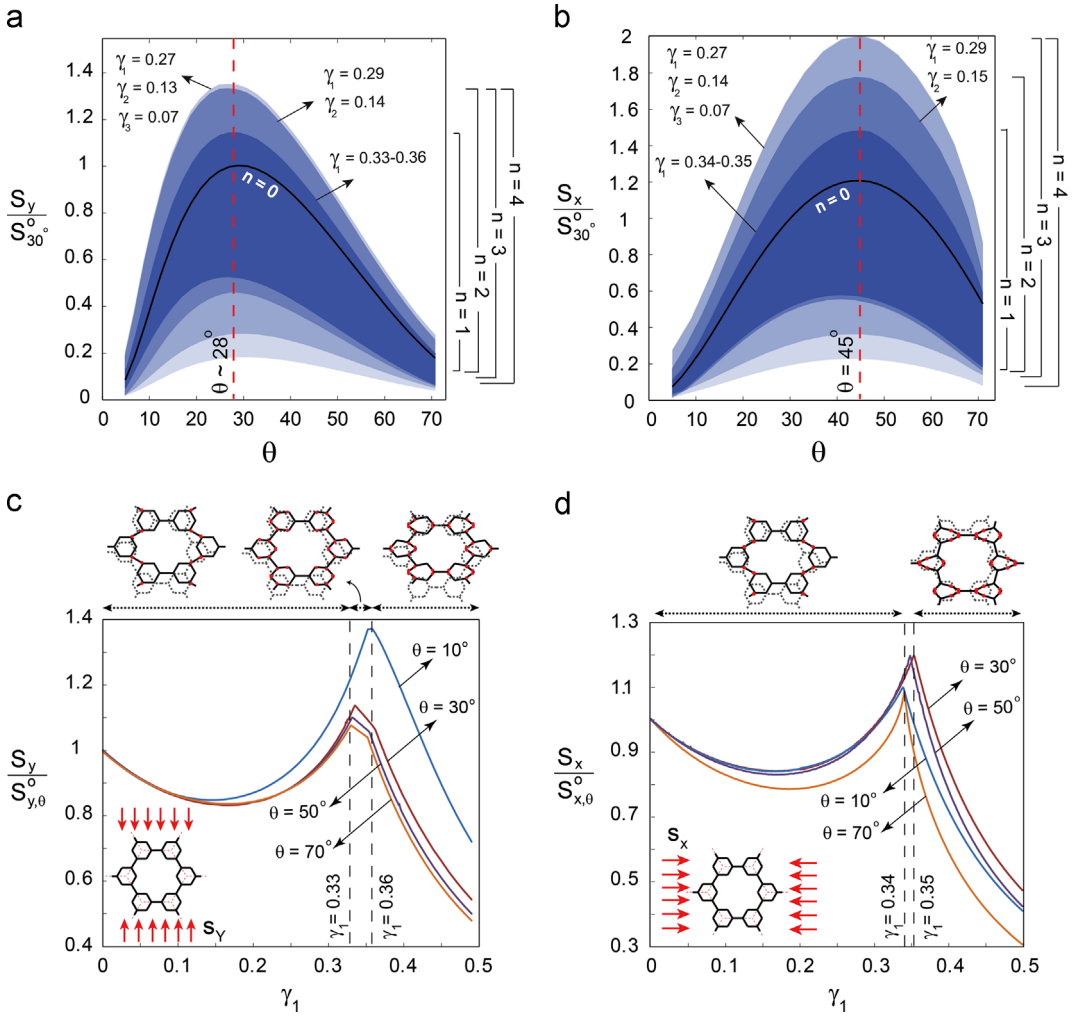

Fig. 7. (a and b) The normalized plastic collapse bandwidth of 1st–4th order hierarchical honeycomb for y and x direction (c and d) The normalized plastic collapse of 1st order hierarchical honeycomb for y and x direction. Plastic collapse mechanisms for different values of γ are shown on the top. Note that for the plastic collapse of structure in y-direction with oblique angle of $\theta = 10^o$, only two mechanisms in left and right are dominant for the whole range of γ. For (a) and (b) the plastic collapse strength is normalized by that of zero order regular honeycomb ($\theta = 30^o$), whereas for (c) and (d) it is normalized by that of zero order honeycomb with same oblique wall angle, θ.

6.3. *Plastic collapse strength*

Fig. 7a and b shows the normalized plastic collapse bandwidth of 1st–4th order hierarchical honeycomb versus oblique wall angle, θ, for y- and x-directions respectively. Here, the plastic collapse strength is normalized by that of zero order regular honeycomb (i.e., $\theta = 30^o$). These two figures show that the maximum achievable plastic collapse strength saturates at the 3rd

order for both y- and x-direction. The maximum plastic collapse strength for different hierarchical orders occurs at approximately $\theta = 28^o$ for y-direction and at $\theta = 45^o$ for x-direction and is nearly independent of hierarchical order. The values of γ at which maximum plastic collapse strength occur in each hierarchical order are virtually independent of θ. For the second order hierarchical structure it was found the maximum x-direction collapse strength occurred when $\gamma_1 = 0.29$, $\gamma_2 = 0.14$ for y-direction and $\gamma_1 = 0.29$, $\gamma_2 = 0.15$ for x-direction. For the third order, the maximum strength was achieved at $\gamma_1 = 0.27$, $\gamma_2 = 0.14$, $\gamma_3 = 0.07$ for both x- and y-direction strengths. The trend in γ values show that by increasing the hierarchical order the edge length of newly generated hexagons tends to be half the edge length of the previous hexagons (i.e., $\gamma_{i+1} = \gamma_i/2$). These results show that the collapse behavior of the hierarchical honeycomb can be improved up to the 3rd order by increasing the hierarchical order. However, further refinement does not make any improvement in collapse strength.

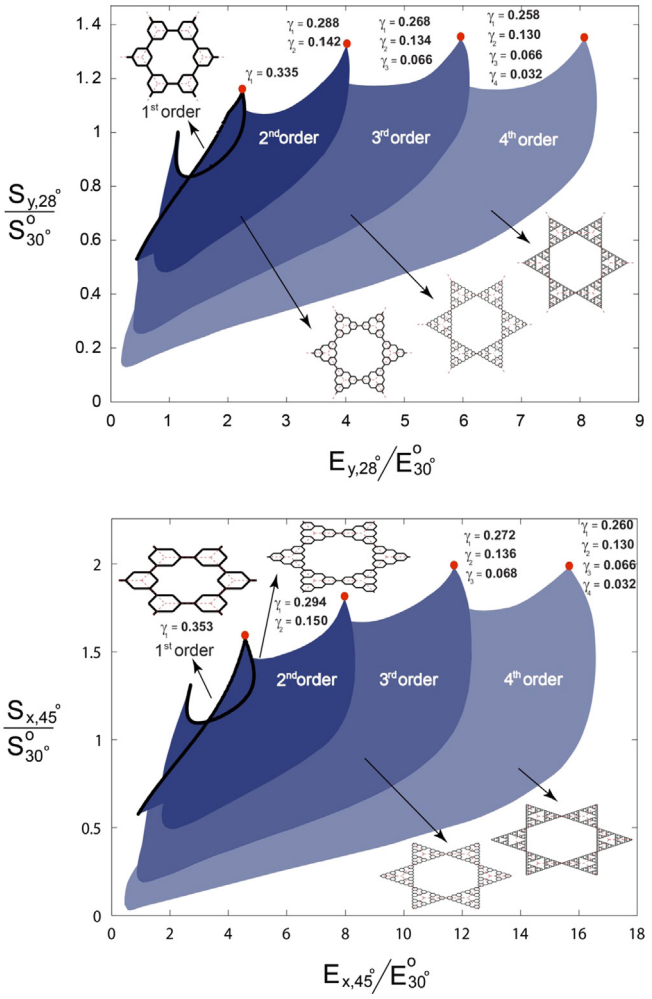

Fig. 8. Plastic collapse strength versus elastic modulus for 1st, 2nd, 3rd, and 4th order hierarchical honeycombs under uniaxial loading for (a) y-direction and $\theta = 28^o$and (b) x-direction and $\theta = 45^o$. The plastic collapse strength and elastic modulus are normalized by those of regular honeycomb of same density. Note that the 1st order is shown by solid line, while higher orders are shown by areas of different shade.

Fig. 7c and d shows the normalized x and y direction plastic collapse strengths of a first-order hierarchical structure versus γ_1 for different values of oblique wall angle, θ. The plastic collapse strength is normalized by that of a zero order honeycomb with same oblique wall angle θ. The results suggest that the γ_1 values corresponding to the maximum normalized plastic collapse strength in x- or y-direction are not fixed for different oblique wall angles. For y direction, the maximum occurs between $\gamma_1 = 0.33 - 0.36$ for the range of oblique beam angle varying between $\theta = 70^o$ and 10^o, while for x direction it occurs between $\gamma_1 = 0.34$ and 0.35 for the same range of angle. For each curve corresponding to a fixed oblique wall angle, θ, there are two points with slope discontinuity for the plastic collapse in the y direction (Fig. 7c), and one point for plastic collapse in the x direction (Fig. 7d). These points represent the locations in which the failure mechanism and the location of plastic hinge points change by increasing the value of γ_1. Corresponding plastic collapse mechanisms and locations of plastic hinges for different range of γ are shown on top of Fig. 7c and d. For the plastic collapse in the y direction as θ decreases, the normalized plastic collapse strength increases. The maximum normalized plastic collapse for $\theta = 10^o$ is equal to 1.37 whereas for $\theta = 70^o$ is equal to 1.08. Fig. 7d shows that $\theta = 30^o$ gives the largest normalized plastic collapse $S_x/S^o_{x,\theta}$ which is equal to 1.2 for the 1st order hierarchy structure.

Having the maximum plastic collapse strength at $\theta = 28^o$ for the y direction and at $\theta = 45^o$ for the x direction suggests a map comparing plastic collapse to elastic modulus. Fig. 8a and b shows the maps of normalized collapse strength versus of normalized elastic modulus for zero to 4th order honeycombs for $\theta = 28^o$ in y direction and for $\theta = 45^o$ in x direction, respectively, obtained from the finite element analysis. It should be noted that an nth order hierarchical honeycomb is a special configuration of honeycombs with higher order of hierarchy. For example, a 1st order hierarchical honeycomb is a special configuration of 2nd order hierarchical honeycombs with, $\gamma_2 = 0$. Thus, the entire colored area in Fig. 8 shows the range of achievable elastic modulus and strength with four orders of hierarchy. Compared to previous data given in [19] for isotropic hierarchical honeycombs, current graphs show a larger range of achievable elastic modulus and plastic collapse strength by stretching the structure in vertical/horizontal direction.

Table 1
Summary of maximum elastic modulus/strength of anisotropic hierarchical honeycombs.

Order		$\overline{E}_x(\theta = 90^o)$	$\overline{E}_y(\theta = 0^o)$	$\overline{G}_{xy}(\theta = 28^o)$	$\overline{S}_x(\theta = 45^o)$	$\overline{S}_y(\theta = 28^o)$
Zero	Value	6.75	6.02	1.02	1.21	1.01
1st	Property value	10.77	11.98	2.86	1.44	1.15
	γ Values	[0.32]	[0.32]	[0.34]	[0.35]	[0.34]
2nd	Property value	17.48	21.20	5.04	1.67	1.27
	γ Values	[0.29, 0.13]	[0.29, 0.13]	[0.30, 0.14]	[0.29, 0.15]	[0.29, 0.14]
3rd	Property value	25.48	32.01	7.87	1.79	1.29
	γ Values	[0.27, 0.13, 0.06]	[0.27, 0.13, 0.06]	[0.27, 0.13, 0.06]	[0.27, 0.14, 0.07]	[0.27, 0.13, 0.07]
4th	Property value	33.92	43.5	10.78	1.79	1.29
	γ Values	[0.26, 0.13, 0.06, 0.03]	[0.26, 0.13, 0.06, 0.03]	[0.26, 0.13, 0.06, 0.03]	[0.26, 0.13, 0.07, 0.03]	[0.26, 0.13, 0.07, 0.03]

Maximum elastic modulus/strength values of anisotropic hierarchical honeycombs, $\overline{E}_x$ for E_x/E^o_{30}, $\overline{E}_y$ for E_y/E^o_{30}, $\overline{G}_{xy}$ for G_{xy}/G^o_{30}, $\overline{S}_x$ for S_x/S^o_{30} and $\overline{S}_y$ for S_y/S^o_{30}.

7. Concluding remarks

Mechanical properties of anisotropic hierarchical honeycombs were investigated, where the term 'anisotropic' represents the change of honeycomb's oblique wall angle by uniform horizontal or vertical stretching of the underlying network, and the term 'hierarchical' represents the replacement of each three-edge vertex of base hexagon structure with a smaller hexagon of same wall angle. The oblique wall angle of the honeycombs and the relative side lengths of newly generated hexagons are two key parameters which determine the stiffness and strength of the structure, at any fixed relative density.

The effective elastic modulus, Poisson's ratio and plastic collapse strength of anisotropic hierarchical honeycombs were obtained as a function of dimension ratios and wall angles of the structure. The analytical results for the elastic part were based on Castigliano's second theorem, and numerical frame analysis was used to validate the analytical approach, and explore higher orders of hierarchy. The results show that a wide range of elastic modulus and strength ratio can be obtained for anisotropic hierarchical honeycombs by varying geometrical parameters. Table 1 summarizes the maximum elastic modulus/strength values of anisotropic hierarchical honeycombs at different hierarchical orders. Increasing the hierarchy order improves the structural performance in terms of its elastic modulus and plastic collapse strength.

Acknowledgments

This work has been supported by the Qatar National Research Foundation (QNRF) under Award number NPRP 09-145-2-061.

Appendix A. Analytical modeling of elastic properties

Elastic modulus in principal directions

we use Castigliano's second theorem [34] to determine analytically the elastic moduli of first and second order hierarchical stretched honeycombs in their principal directions. The cell walls of thickness t consist of an isotropic elastic material with elastic modulus E_s, Poisson's ratio ν_s and yield stress σ_Y. Since a conventional hexagonal network extending to infinity has six-fold rotational symmetry, any linear second order tensorial operator (e.g., thermal conductivity) or linear fourth-order operator (e.g., elastic modulus) must be isotropic. However when anisotropy is present, the resulting 'material' has only two-fold rotational symmetry, and an orthotropic elasticity tensor. The macroscopic in-plane elastic behavior of an orthotropic material can be described by 5 constants (i.e., $E_x, E_y, \nu_{xy}, \nu_{yx}$ andG_{xy}) , of which four are connected by the *reciprocal relation* [35]: $E_x\nu_{yx} = E_y\nu_{xy}$. Here E_x and E_y are the elastic moduli in the x and y directions normalized by material elastic modulus E_s, and ν_{xy} and ν_{yx} are orthotropic Poisson's ratios in the x and y directions, defined as (−strain in second index direction)/(strain in first index direction) due to uniaxial stress in first index direction. Thus, for network angles other than 30°, instead of two elastic constants governing in-plane deformation, the structure has four.

For the analytical investigation, each cell wall is treated as an Euler–Bernoulli beam, and the stored bending energy is evaluated based on the loading conditions. The modulus is determined from unit-cell boundary point displacements. Following [18], the far-field uniaxial stresses $\sigma_{yy} = -F/(3l_0 \sin(\theta))$ or $\sigma_{xx} = -P/(l_0 \cos(\theta))$ were imposed to determine the y- and x-direction elastic moduli, where l_0 is the oblique wall length of the underlying zero-order honeycomb, and θ is the oblique wall angle. Vertical stress is equivalent to applying a vertical force F at every cut point of a horizontal line passing through the mid-points of oblique edges in a row of underlying (i.e., no hierarchy) hexagons (such as points H and H' in Fig. 1a). Horizontal stress is equivalent to applying a horizontal force P at every cut point of a vertical line passing through the midpoints of oblique edges in a row of underlying (i.e., no hierarchy) hexagons (such as points V, V', V'' and V''' in Fig. 1a). Due to 180° rotational symmetry, these cut points are moment-free for any choice of uniform remote stress components (i.e., σ_{yy}, σ_{xx} and τ).

Fig. 2b shows a unit cell with 1st order hierarchy subjected to both vertical (σ_{yy}) and horizontal loading (σ_{xx}), however in this section they are analyzed separately. Due to the geometrical and force symmetry, we may apply Castigliano's method to a reduced subassembly, namely the upper half of the unit cell. For loading in the x- and y-directions, point 4 is subjected only to force $-P$ in the x direction or force $-F$ in the y direction. (For shear loading, to be considered later, the bottom half of the unit cell is also needed, as shown with dotted lines, and non-symmetrical forces as shown are also required.) Due to the structural symmetry, point 3 is clamped for all the analysis [18]. At the subassembly centerline cut points 1 and 2, the y-direction forces acting on the upper subassembly are denoted by N_1 and N_2, and moments are denoted by M_1 and M_2. There can be no horizontal force acting on the upper half-assembly at point 1 because of reflection symmetry about the x axis.

For the first order hierarchy, the elastic bending energy stored in the statically indeterminate subassembly can be expressed as a function of the external force F or P, and the force and moment N_1 and M_1, applied to the structure at point 1: $U(F \text{ or } P,\ M_1,\ N_1) = \sum_{all\ beams} \int (M^2/(2E_sI))ds$. Here M is the bending moment at the location s along a cell wall, and I is the beam's area moment of inertia, which is constant because of the uniform-thickness refinement. To simplify the analysis, we have assumed the normalized structural density to be so low that all macroscopic deformations can be attributed solely to bending of cell walls. (Effectively, axial and shear stiffness are taken to be infinite.)

Assuming zero vertical displacement and zero rotation at points 1, 3, and also along the horizontal beam connecting points 2 and 3 (due to symmetry), N_1 and M_1 can be obtained from $\partial U/\partial N_1 = 0$ and $\partial U/\partial M_1 = 0$. These two relations allow N_1 and M_1 to be expressed algebraically in terms of F for vertical loading, or P for horizontal loading. The displacements δ_y at the point 4 can then be found from $\delta_y = \partial U(F)/\partial F|_{N_1,M_1}$ and $\delta_x = \partial U(P)/\partial P|_{N_1,M_1}$, which allows to obtain strains in the principal directions of structure (for evaluating Poisson's ratio, both F and P should be applied simultaneously).

For the second order of hierarchy, elastic energy in the section model of Fig. 2c is obtained as a function of the external force F or P, and unknown reaction forces and moments N_1, M_1, N_2 and M_2 at points 1 and 2: $U = U(F \text{ or } P,\ N_1,\ M_1, N_2, M_2) = \sum_{all\ beams} \int (M^2/(2E_sI))dx$ (where N_3 and M_3 can be written as functions of N_1, M_1, N_2, M_2 and F or P by means of the equilibrium equations). N_1, M_1, N_2 and M_2 are obtained by invoking the concept of the least work: $\partial U/\partial N_1 = 0$, $\partial U/\partial M_1 = 0$, $\partial U/\partial N_2 = 0$ and $\partial U/\partial M_2 = 0$. Similar to the first order hierarchy, point 4 is clamped for all the analysis [18].

Shear modulus

To obtain the shear modulus, we imposed far-field shear stress τ, which gave rise to forces $P = -\tau(3l_0 \sin\theta)$ below the horizontal cut HH′, and forces $F = -\tau(l_0 \cos\theta)$ to the left of vertical cut VV′ in Fig. 1a. In a state of pure shear stress, $P = 3F \cdot tan(\theta)$. Since the loading is not symmetric with respect to the unit cell midline, the

full subassembly of Fig. 2b and c must be analyzed to find the stored bending energy.

Using the same procedure as above, the bending energy stored in a first order hierarchical structure can be expressed as a function of the simultaneously applied external forces F and P: $U = U(F,\ P)$. The bending moments along each side of the complete hexagon are determined from a subsidiary analysis in which it is divided at nodes 5 and 6, and then three compatibility conditions are enforced at each of those nodes [18]. Displacements δ_y and δ_x at point 4 can be found from: $\delta_y = \partial U(F,\ P)/\partial F$ and $\delta_x = \partial U(F,\ P)/\partial P$.

Poisson's ratio

To obtain the dependence of the orthotropic Poisson's ratios on the dimension ratio of the hierarchical structure, we again used Castigliano's second theorem and analyze the upper half of the Fig. 2 subassembly. We determined ν_{yx} only, since $E_x\nu_{yx} = E_y\nu_{xy}$ allows to find ν_{xy}. Applying far-field stress $\sigma_{yy} = -F/\ (3l_0\ \sin(\theta))$ in a vertical direction is equivalent to applying a vertical force F at point 4 of Fig. 2b for first order hierarchy and at point 5 of Fig. 2c for second order hierarchy. Here we apply the dummy horizontal force P which allows using Castigliano's theorem to find the horizontal displacement of the node. When P is zero, the x and y displacements of the upper node due to force F can be expressed as follows: $\delta_x = (\partial U/\partial P)|_{N_1,M_1,P=0}$ and $\delta_y = (\partial U/\partial F)|_{N_1,M_1,P=0}$, where U is the bending energy stored in the structure due the forces F and P.

References

[1] Katz JL, Misra A, Spencer P, Wang Y, Bumrerraj S, Nomura T, et al. Multiscale mechanics of hierarchical structure/property relationships in calcified tissues and tissue/material interfaces. Mater Sci Eng: C 2007;27:450–68.

[2] Fratzl P, Weinkamer R. Nature's hierarchical materials. Prog Mater Sci 2007;52:1263–334.

[3] Barthelat F, Tang H, Zavattieri P, Li CM, Espinosa H. On the mechanics of mother-of-pearl: a key feature in the material hierarchical structure. J Mech Phys Solids 2007;55:306–37.

[4] Yao H, Gao H. Mechanics of robust and releasable adhesion in biology: bottom-up designed hierarchical structures of gecko. J Mech Phys Solids 2006;54:1120–46.

[5] Ren D, Ma Y, Li Z, Gao Y, Feng Q. Hierarchical structure of asteriscus and in vitro mineralization on asteriscus substrate. J Cryst Growth 2011;325:46–51.

[6] Aizenberg J, Weaver JC, Thanawala MS, Sundar VC, Morse DE, Fratzl P. Skeleton of Euplectella sp.: structural hierarchy from the nanoscale to the macroscale. Science 2005;309:275–8.

[7] Qing H, Mishnaevsky Jr L. 3D hierarchical computational model of wood as a cellular material with fibril reinforced, heterogeneous multiple layers. Mech Mater 2009;41:1034–49.

[8] Su Y, Ji B, Zhang K, Gao H, Huang Y, Hwang K. Nano to micro structural hierarchy is crucial for stable superhydrophobic and water-repellent surfaces. Langmuir 2010;26:4984–9.

[9] Lakes R. Materials with structural hierarchy. Nature 1993;361:511–5.

[10] Baer E, Hiltner A, Keith H. Hierarchical structure in polymeric materials. Science 1987;235:1015–22.

[11] Russell B, Deshpande V, Fleck N. The through-thickness compressive strength of a composite sandwich panel with a hierarchical square honeycomb sandwich core. J Appl Mech 2009;76:1004.

[12] Kazemahvazi S, Zenkert D. Corrugated all-composite sandwich structures. Part 1: modeling. Compos Sci Technol 2009;69:913–9.

[13] Kazemahvazi S, Tanner D, Zenkert D. Corrugated all-composite sandwich structures. Part 2: failure mechanisms and experimental programme. Compos Sci Technol 2009;69:920–5.

[14] Deshpande V, Wadley HNG. Hierarchical corrugated core sandwich panel concepts. J Appl Mech 2007;74:259.

[15] Fan H, Jin F, Fang D. Mechanical properties of hierarchical cellular materials. Part I: analysis. Compos Sci Technol 2008;68:3380–7.

[16] Zhang Z, Zhang YW, Gao H. On optimal hierarchy of load-bearing biological materials. Proc R Soc B: Biol Sci 2011;278:519–25.

[17] Tang Z, Kotov NA, Magonov S, Ozturk B. Nanostructured artificial nacre. Nat Mater 2003;2:413–8.

[18] Ajdari A, Jahromi BH, Papadopoulos J, Nayeb-Hashemi H, Vaziri A. Hierarchical honeycombs with tailorable properties. Int J Solids Struct 2012;49:1413–9.

[19] Haghpanah B, Oftadeh R, Papadopoulos J, Vaziri A. Self-similar hierarchical honeycombs. Proc R Soc A: Math Phys 2013;469:5322–34.

[20] Haghpanah B, Chiu S, Vaziri A. Adhesively bonded lap joints with extreme interface geometry. Int J Adhes Adhes 2014;48:130–8.

[21] Chen Q, Pugno NM. In-plane elastic buckling of hierarchical honeycomb materials. Eur J Mech-A/Solids 2012;34:120–9.

[22] Ajdari A, Nayeb-Hashemi H, Vaziri A. Dynamic crushing and energy absorption of regular, irregular and functionally graded cellular structures. Int J Solids Struct 2011;48:506–16.

[23] Vaziri A, Xue Z, Hutchinson JW. Performance and failure of metal sandwich plates subjected to shock loading. J Mech Mater Struct 2007;2:1947–63.

[24] Vaziri A, Xue Z. Mechanical behavior and constitutive modeling of metal cores. J Mech Mater Struct 2007;2:1743–61.

[25] Wadley HNG, Dharmasena KP, Queheillalt DT, Chen YC, Dudt P, Knight D, et al. Dynamic compression of square honeycomb structures during underwater impulsive loading. J Mech Mater Struct 2007;2:2025–48.

[26] Zheng Z, Yu J, Li J. Dynamic crushing of 2D cellular structures: a finite element study. Int J Impact Eng 2005;32:650–64.

[27] Lu T, Chen C. Thermal transport and fire retardance properties of cellular aluminium alloys. Acta Mater 1999;47:1469–85.

[28] Vaziri A, Hutchinson JW. Metal sandwich plates subject to intense air shocks. Int J Solids Struct 2007;44:2021–35.

[29] Rathbun H, Radford D, Xue Z, He M, Yang J, Deshpande V, et al. Performance of metallic honeycomb-core sandwich beams under shock loading. Int J Solids Struct 2006;43:1746–63.

[30] Vaziri A, Xue Z, Hutchinson JW. Metal sandwich plates with polymer foam-filled cores. J Mech Mater Struct 2006;1:97–127.

[31] Xue Z, Hutchinson JW. Crush dynamics of square honeycomb sandwich cores. Int J Numer Methods Eng 2006;65:2221–45.

[32] Xue Z, Hutchinson JW. A comparative study of impulse-resistant metal sandwich plates. Int J Impact Eng 2004;30:1283–305.

[33] Logan DL. A First Course in the Finite Element Method. United States: Brooks, Cole Thomson learning; 2002.

[34] Boresi AP, Schmidt RJ, Sidebottom OM. Advanced mechanics of materials. New York: Wiley; 1993.

[35] Gibson LJ, Ashby MF. Cellular solids: structure and properties. Cambridge University Press; 1999.